CPT 186
ORO-3992-137

"Absorbed Multiperipheral-like Model of Elastic Scattering and Multiparticle Production In High Energy Hadron Collisions"*

by

Charles B. Chiu

and

Kuo-Hsiang Wang

Center for Particle Theory
University of Texas
Austin, Texas 78712

*Work supported in part by the USAEC (40-1)3992.

ABSTRACT

We present an overall picture for hadron collisions extracted from some of our recent extensive work based on the absorbed multiperipheral-like model with an independent emission parameterization. This model accounts for a number of observed features in the multiparticle production and elastic scattering of pp collisions. The multiparticle data considered are: pion multiplicity distribution, pion and nucleon inclusive transverse momentum distributions and the moments of the inclusive longitudinal distribution. And the elastic data are: total cross section, ratio of the real part to the imaginary part of forward amplitude and d fferential cross section.

The model we would like to consider in this paper is an extract of our recent extensive work based on the absorbed multiperipheral-like model with independent emission parameterization.[1,2,3] Many features of the elastic and multiparticle production data have been incorporated in the model.

1. Motivation of the model.

We recall some common features of the two well known models for multiparticle production: the multiperipheral model[4] and the uncorrelated jet model[5] (or the independent emission model[6]). For the former, in its simplest form, particles (say pions) are produced along the multiperipheral chain. The 2 to n + 2 production amplitude has a factorizable momentum transfer-squared dependence. With a sharp cutoff in momentum-transfer, this model predicts a similar cutoff in transverse momentum for pions produced. Also, it predicts a Poisson shape for the multiplicity distribution:

$$\sigma_n \sim \frac{(\bar{n})^n}{n!} \quad , \qquad \text{with } \bar{n} \sim g^2 \ln s \quad , \tag{1}$$

where g^2 is some effective coupling constant, and a power behavior in s for the total production cross section

$$\sigma_{in} = \sum_n \sigma_n \sim s^{\epsilon+g^2} = s^c \quad . \tag{2}$$

In Eq. (2), if the model is generalized to include the exchanges of the Regge trajectory with an intercept α, the power $\epsilon = 2\alpha - 2$.

On the other hand, for the independent emission model, one assumes that particles produced are essentially uncorrelated among themselves, except for the conservation laws, such as the conservation of charge and the conservation of four-momentum. In this model each particle emitted is assumed to have a sharp transverse momentum cutoff. In particular the transverse-momentum-dependent part of the 2 to n + 2 amplitude has the factorizable form,

$$T_{n+2,2} \propto \prod_{i=0}^{n+1} f(p_{iT}) \quad . \tag{3}$$

Treating the particles produced in a statistical manner, in this model the multiplicity distribution is again given by a Poisson distribution with its average multiplicity $\bar{n}$ proportional to $\ln s$, thus again arrives at Eq. (1). Furthermore, if one makes the added assumption that for the overall normalization of σ_n there is a factor s^{ϵ}, this leads to Eq. (2). Following ref. 2, we shall again refer to those models which have the following three features as multiperipheral-like (MP-like) models: a) a sharp cutoff in the transverse momenta of final products; b) a Poisson (or Poisson-like) multiplicity distribution with $\bar{n} \sim \ln s$; and c) a power behavior for the inelastic production cross section.

A simple MP-like model with the direct production of pions is known to be inadequate, at least on two accounts. Firstly, the ISR data[7] show a rising total cross section. From property c), to reproduce an asymptotic rise in the total cross section,

it would require a positive power, i.e., in Eq. (2), $c > 0$. This violates Froissart bound. Secondly, the pion multiplicity distribution data at high energies (e.g. beyond 100 GeV/c^8) is not compatible with the distribution predicted by the direct emission of pions. The width of the observed distribution is too broad compared to this prediction. To explain the data, some correlation effects, at least among the pions, are needed.[1,9] We shall show that both of these difficulties can be resolved by the inclusion of some plausibly expected "nonproductive-type" of interactions. And we shall explore these interactions with the independent-emission-model parameterization of Eq. (3). Our choice of this parameterization is mainly motivated by the fact, that there has been difficulty with the corresponding multiperipheral-model parameterization for achieving a consistent description of the diffractive peak and the inclusive p_T-distribution data.[10] Similar difficulty does not arise with Eq. (3).

We consider the production process: $pp \to NN + \pi\pi\cdots$, and assume for the time being pions are emitted via some MP-like production mechanism. Due to the character of strong interactions, it is plausible that there should be further non-productive-type interactions:

I - among the pions,

II - between the pions and each of the two nucleons,

and III - between the two nucleons.

Type I is expected to be important, when the energy of some subsystem of pions is low. Here with an appropriate quantum

number, a meson-resonance can be formed. Similar to the approaches of others,[9] we shall crudely account for this by altering the original assumption to allow the uncorrelated emissions of meson-resonances in addition to pions. Analogously, type II is accounted for by allowing the presence of nucleon resonances and also nucleon "clusters" (or the target- and the projectile- fragmentations). For type III, we motivate the effect involved by a geometric picture.[11] Consider two protons with extended structure passing through each other in the c.m. frame. First look at the elastic scattering case. The interaction between the two "nucleon-systems" at an impact parameter b and energy s is characterized by the corresponding phase shift $\delta_{22}(b,s)$. For the case of multiparticle production, denote the c.m. longitudinal momentum of the projectile nucleon, the relative impact parameter and energy squared of the two nucleons at the initial state and the final state by p_L,b,s and p_L',b',s' respectively. At high energies, on average p_L' maintains a substantial fraction of the incident momentum (this is the well known leading particle effect, e.g. at 102 GeV/c, $p_L'/p_L \approx 0.7$). So the final two-nucleon system is still expected to be at relatively high energy. With the experimental facts: the c.m. longitudinal momenta of pions are relatively small and pions have a characteristic p_T-cutoff function similar to that of the nucleon, it can be shown[3] that the pion production does not alter the relative impact parameter of the two nucleons significantly. So b' does not deviate significantly from its initial value, b.

Define the mean relative impact parameter and the mean energy of the two nucleon-systems averaging over the entire overlapping process to be $\bar{b}$ and $\bar{s}$ (where $\bar{b}$ is bounded by b and b' and $s' < \bar{s} < s$). We make the crucial assumption that in the presence of production, the phase shift due to the interaction of the two nucleon-systems is essentially the same as the elastic phase shift. So for n-pion production, this phase shift is given by

$$\delta_{22}^{(n)}(\bar{b},\bar{s}) = \delta_{22}(\bar{b},\bar{s}) \simeq \delta_{22}(b,s) \quad . \tag{4}$$

We proceed to explain the approximation of the last step. In the high energy region of interest, the data indicate that the elastic amplitude varies very slowly with energy, and the phase shifts have a very weak energy dependence. We have seen already that s', and in turn $\bar{s}$, still corresponds to high energy, so $\delta_{22}(\bar{b},\bar{s}) \simeq \delta_{22}(\bar{b},s)$. We have also mentioned the fact that b', and in turn $\bar{b}$, does not deviate significantly from b. This leads to the approximation in Eq. (4). So we shall assume that at given initial values of b and s, the phase shift due to the two nucleon interaction in the presence of multiparticle production is the same as that for the elastic scattering and propose that the multiparticle production amplitude is given by

$$\tilde{T}_{n+2,2}(b) = \tilde{T}^{B}_{n+2,2}(b)\ \tilde{S}_{22}(b) \quad , \tag{5}$$

where in the arguments the energy dependence and detail specifications of the n + 2 particles in the final state are suppressed. The symbol "~" stands for functions in the impact parameter space. In general a t-dependent function and its corresponding function in the impact parameter space is related by a Fourier-Bessel transform defined by

$$\langle \psi(x) \rangle_y = \int_0^\infty x dx \, J_0(xy) \psi(y) \quad , \tag{6}$$

where J_0 is the zeroth order Bessel function of the first kind. For example,

$$\tilde{S}_{22}(b) = \langle S_{22}(t) \rangle_b \quad , \qquad S_{22}(t) = \langle \tilde{S}_{22}(b) \rangle_{\sqrt{-t}} \quad , \text{ etc.} \tag{7}$$

The S-matrix $\tilde{S}_{22}(b)$ has a behavior crudely resembles that of a grey disk. The absorption defined in Eq. (5) modifies the unabsorbed amplitude most significantly in the small b region. In this region, $\tilde{S}_{22}$ varies very slowly with b. This lends an extra support for the approximation used in Eq. (4).

To conclude, we remark that with the inclusion of the effects of the nonproductive-type of interactions discussed, one can indeed cure the two inadequacies of the simple MP-like model mentioned earlier. In particular, types I and II will provide correlations needed for the multiplicity distribution, while type III corresponds to an absorption mechanism, which together with a positive power ($c > 0$ in Eq. (2)), will enable one to describe a rising total cross section and at the same time preserve Froissart bound.

2. The model

With those features of the MP-like model and effects of the nonproductive interaction described in the previous section in mind, we suggest the following model for pp collisions. (It is a straight-forward matter to generalize this model to other reactions, but we will not go into this here.) We idealize the production process of pp interaction to be of the form:

$$\begin{aligned} &\text{A. } pp \to NN + \text{pions} + \text{meson resonances}, \\ &\text{B. } pp \to NN^* + \text{pions} + \text{meson resonances}, \\ &\text{and C. } pp \to N^*N^* + \text{pions} + \text{meson resonances}, \end{aligned} \tag{8}$$

where N^* denotes the nucleon resonances and also nucleon clusters. We shall loosely refer all those final state objects in (8) as "particles".

The key assumptions of our proposal are as follows.

Ansatz I. The physical process for particle production is described by the absorbed amplitude of the form of Eq. (5).

Ansatz II. The unabsorbed amplitude $T^B_{n+2,2}$ is specified by the MP-like model with the independent emission parameterization, where pions and meson resonances in (8) are independently produced. More specifically, the general form of the p_T-cutoff function for particles produced is given in Eq. (3) and that of the particle multiplicity distribution is detailed in Eq. (12) below.

Ansatz III. The absorptive part of the two-body diffractive amplitude which dominates at high energies is assumed to be crossing even and it is assumed to be built up through the

unitarity relation,

$$2\ \mathrm{Im}\ \tilde{T}_{22} = |\mathrm{Im}\ \tilde{T}_{22}|^2 + |\tilde{S}_{22}|^2\ \tilde{H} \quad , \tag{9}$$

where the relation is given in the b-space and $\tilde{H}$ is the unabsorbed overlap function. As usual, this overlap function in terms of the momentum transfer square t, is defined by

$$H(t) = \sum_n \int d\phi'_{n+1}\ T^{B*}_{n+2,2}(p'_a;p'_i)T^{B}_{n+2,2}(p_a;p'_i) \quad , \tag{10}$$

where p_a and p'_a are the four-momenta of the initial and the final projectile-nucleon in the c.m. system, and $t = (p_a - p'_a)^2$, p_i's are the momenta of intermediate particles with $i = 0,1,2\cdots n+1$. The integral is over the phase space of the intermediate state. From Eq. (7),

$$\tilde{H}(b) = \langle H(t) \rangle_b \quad . \tag{11}$$

For the remaining of this section, we shall discuss the specific parameterizations for the multiplicity distribution and the cutoff function. And will present the applications of the model to the elastic scattering data in Sec. 3, and to the inclusive p_T-distribution data in Sec. 4.

The assumption of independent emission of particles (ansatz II) leads to the following form for the multiplicity distribution,

$$\sigma_{[n_i]} \sim \pi_{[n_i]} \frac{(\bar{n}_i)^{n_i}}{n_i!} e^{-\bar{n}_i} \quad , \tag{12}$$

with

$$\bar{n}_i = g_i^2 \, \ell n(s/s_i) \quad , \tag{13}$$

where n_i denote the number of i-type specy. Conservation of charge imposes the constraint, $\sum_i n_i Q_i = 0$, with Q_i being the charge of the i-type specy. From the knowledge of particle decay modes, it is a straight-forward matter to deduce the corresponding pion multiplicity distribution.[1]

In ref. 1, we have considered the effect due to the uncorrelated emissions of all prominent meson resonances up to 1300 MeV (σ, ρ, ω, A_1, A_2, f and B). So far the π^- multiplicity distribution is concerned, without loss of generality, the distribution can be represented by the emission of π and two effective resonances, for example those having the quantum number and the decay modes of σ and B. The experimental data of the pion multiplicity distribution are presented in the form of the "diffractive" and the "nondiffractive" components, with latter being dominating.[6b] We assumed that this component is given by process-A of (8) and found that the data available can in fact be fitted from 20 GeV/c up by the independent emission of π and B alone, with the average particle multiplicities[1]

$$\bar{n}_\pi = 0.26 \, \ell ns + 3.42 \quad , \tag{14}$$

$$\text{and } \bar{n}_B = 0.65 \, \ell ns - 2.00 \quad .$$

It is important to note that $\bar{n}_\pi$ and $\bar{n}_B$ are indeed linear in $\ell n s$ which supports Eq. (13), or ansatz II. In ref. 2 we have shown that absorption mechanism of ansatz I essentially does not affect the multiplicity distribution, except for an overall normalization. So Eq. (12) actually represents a general form for the absorbed multiplicity distribution within our proposal. And the work of ref. 1 shows that the detail multiplicity distribution data are consistent with the present scheme.

For the calculation of the elastic amplitude and the inclusive distribution, we shall approximate the entire production processes by the dominating process, the process-A of (8) and assume the very form of Eq. (3) for the transverse momentum dependence. In other words, for the latter we assume the cutoff functions of pions, meson resonances and protons are the same. This is mainly for simplicity, although some crude resemblance of the various distributions is also suggested by the data. Of course in the future when more accurate data are available, one can always come back to include all those three processes of (8) and have more refined cutoff expressions.

For the cutoff function, we choose the form

$$\tilde{f}(b) = \left[\frac{B_1(1 + \lambda_1\sqrt{b^2 + B_1^2})}{(b^2 + B_1^2)^{3/2}}\right]^{1/2} \exp\left[\frac{-\lambda_1}{2}(\sqrt{b^2 + B_1^2} - B_1)\right], \quad (15)$$

with

$$f(p_T) = \langle \tilde{f}(b) \rangle_{p_T} .$$

This cutoff function enables us to obtain a simple form for the corresponding unabsorbed overlap function with a desirable t-channel square-root threshold branch cut. In particular, from Eqs. (3), (10) and (15), we obtain[3]

$$H(t) \simeq FE^{C}\, G(t) \quad , \tag{16}$$

with

$$G(t) \simeq \exp\left[-2B_1 \bar{x}_N (\sqrt{-t + \lambda_N^2} - \lambda_N)\right] \quad , \tag{17}$$

where $\lambda_N = \lambda_1/\bar{x}_N$, and $\bar{x}_N$ is the rms moment of the inclusive x-distribution for nucleon. Notice that the pion contribution does not enter in the overlap function at all, this is related to the smallness of the rms value of the moment, $\bar{x}_\pi$. Typically for example at 102 GeV/c, for the pions the rms value $\bar{x}_\pi = 0.04$, while for nucleons the mean value $\tilde{x}_N = 0.7$. From the general shape of the x-spectra, one expects the rms value $\bar{x}_N > 0.7$. We shall discuss the effect of the square root branch point in Eq. (17) later.

3. Comparision with the elastic data.

Approximating $\tilde{T}$ to be purely imaginary and remembering $\tilde{S} = 1 + i\tilde{T}$, we solve the unitarity equation, Eq. (9), and get

$$\text{Im } \tilde{T}_{22} = 1 - \frac{1}{\sqrt{1 + H}} \quad . \tag{18}$$

Imposing the crossing even condition of ansatz III, we make the usual replacement of E by $Ee^{-i\pi/2}$ in $\tilde{T}_{22}$. The elastic amplitude becomes

$$\vec{T} = i\left[1 - \frac{1}{\sqrt{1 - 2i\vec{T}_o}}\right] \quad , \qquad \text{with } \vec{T}_o = \frac{i}{2} F\,(Ee^{-i\pi/2})^c\, G(t). \tag{19}$$

The total cross section, differential cross section and the slope parameters are respectively given by

$$\sigma_T = 4.89 \text{ Im } T \qquad \text{(in mb)} \quad ,$$

$$\frac{d\sigma}{dt} = 1.22|T|^2 \qquad \text{(in mb/GeV}^2\text{)} \quad , \tag{20}$$

$$\text{and } B = \frac{d}{dt} \ell n \frac{d\sigma}{dt} \quad ,$$

where $T = \langle \tilde{T}(b) \rangle_{\sqrt{-t}}$.

To compare with the data, we have added a background term. This is chosen to be a standard Regge-pole term[A] with a nominal Regge trajectory $\alpha(t) = \frac{1}{2} + t$. At high energies, this term is suppressed by a factor $s^{-1/2}$ in the amplitude and is relatively small, say beyond 100 GeV/c. We have fitted

the available elastic data:[12,13] the total cross section, the ratio Re/Im at t = 0, the slope parameters and some sample differential cross sections ranging from 12.8 to 1500 GeV/c. The parameters obtained are

$$F = 24.3\ \text{GeV}^{-2}\ , \qquad c = 0.09\ ,$$
$$B_N = 2.97\ \text{GeV}^{-1}\ , \quad \text{and} \quad \lambda_N = 0.43\ \text{GeV}\ . \tag{21}$$

Some sample fits to the data are shown in Figs. 1, 2 and 3. In these figures, all the curves for the present model are labelled as "I" and are referred to as the independent emission case (IE case). The curves computed with the multiperipheral model parameterization for the momentum-transfer-square dependence are "II" and referred to as the MP case. They are also included for comparison. Earlier we mentioned that the MP case cannot give a simultaneous description to both the elastic and the inclusive data. We will not elaborate on this case except referring the reader to ref. 2. Fits to the differential cross sections for both cases are satisfactory up to $|t| = 0.8\ \text{GeV}^2$, we also refer the reader to ref. 2 for illustrations.

Several comments on the parameters of the solution are in order. The parameter c is positive due to the constraint of the rising total cross section data (see Fig. 1). The magnitude of c together with λ_N governs the rate of this rise.

At ultra high energies (beyond the Isabelle energy 8×10^4 GeV), the leading asymptotic behavior is given by $\sigma_T \sim 2.45\, c^2(\ell nE)^2/\lambda_N^2 = 0.11(\ell nE)^2$.

Notice without absorption, the slope parameter of the asymptotic differential cross section would be independent of s. After the absorption, a mild increase of this parameter as function of s is resulted. This together with the background term gives a good fit to the data up to ISR energies shown in Fig. 2. Also as mentioned earlier, the overlap function defined by Eqs. (16) and (17) has a branch cut in t. This cut starts at $t = \lambda_N^2$, where λ_N is the effective t-channel low mass thresholds with vacuum quantum number. From Eq. (21), $\lambda_N \sim 3m_\pi$, which is quite satisfactory. Furthermore the presence of this nearby t-channel singularity causes a noticeable change in the slope of the differential cross section, in accord with the data. The comparison between the theoretical curves and the data for the slope parameters at $t = 0$ and $t = -0.325$ is shown in Fig. 2. One can see the agreement at high energy is reasonable.

Fig. 3 illustrates the ratio of the real part to the imaginary part of the elastic amplitude at $t = 0$. With the crossing-even assumption of ansatz III, the present diffractive amplitude predicts that this ratio should be positive. The negative value in the low energy region is due to the background contribution. Notice that as the energy increases the data show the trend of a sign change. This lends an extra support for the crossing-even assumption.

4. The inclusive data.

To further test the consistency of our proposal, we have made a parameter free prediction for the inclusive distribution.[3] The expression for this distribution is somewhat involved due to the fact that the inclusive particle is in a plane wave state which is a superposition of infinite angular momentum states. Thus even after the angular momentum of the remaining n + 1 particles is specified, the total angular momentum of the overall n + 2 particles can still be arbitrary. Consider the unitarity diagram for the inclusive calculation shown in Fig. 4. From the discussion above, clearly there are a number of integrations involved, which correspond to double summations over the angular momenta b_x and b'_x of the inclusive particle and the summations over angular momenta of the remaining (n + 1)-particle system. In general, each summation corresponds to a two-dimensional integral due to magnetic quantum number involved. Within our approximation, because of the smallness of $\bar{x}_\pi$, the angular momenta of pions are always small and then ignored. For nucleon inclusive distribution, there is only one nucleon in the (n + 1)-particle system, in turn, a single summation over the nucleon angular momentum b". Conservation of angular momentum gives the approximate relation[3,10a] $\underset{\sim}{b} = \bar{x}_N(\underset{\sim}{b}_x + \underset{\sim}{b}")$. The inclusive distribution for the proton is found to be given by,[3]

$$\frac{d\sigma}{dp_T^2} \sim \int d^2b" |\tilde{f}(b")|^2 \cdot \left| \int db_x^2 \, \tilde{f}(b_x) e^{-i\underset{\sim}{p}_T \cdot \underset{\sim}{b}_x} S_{22}(\bar{x}_N(\underset{\sim}{b}_x + \underset{\sim}{b}")) \right|^2 , \tag{24}$$

The prediction for the nucleon inclusive p_T-distribution, obtained from the parameters of Eq. (21) and a typical value $\bar{x}_N \simeq 0.9$, is shown as the solid curve in Fig. 5 together with the data points[14] for comparison. Although this curve appears to be somewhat sharper than the trend of data in the small p_T region, as a whole, considering it being a parameter-free prediction, the curve does reproduce the gross trend of the data reasonably well.

For the pion inclusive distribution, it is found[3] that

$$\frac{d\sigma}{dp_T^2} \sim |f(p_T)|^2 \cdot \int d^2b'_N |f(b'_N)|^2 \int d^2b_N |f(b_N)|^2 \cdot |S_{22}(\bar{x}_N(b_N + b'_N))|^2 \tag{25}$$

$$\propto |f(p_T)|^2 \quad .$$

Notice in the integrand, there are two summations over the nucleon angular momenta b_N and b'_N, since both nucleons now belong to the remaining (n + 1)-particle system. As mentioned previously within our approximation, the pion angular momentum is ignored. So the pion distribution is unaffected by the b-dependent absorption effect. Thus the absorption only amounts to changing the overall normalization. The pion data (the curve with crosses) and the theoretical prediction with the assumed universal cutoff function (the dashed curve) are also shown in Fig. 5. The agreement between the theory and the data is reasonable.

5. Discussion.

Let us recapitulate the essence of the model we considered. In this model, proton-proton collisions at high energies are associated with the following production picture. Here pions and meson-resonances are independently emitted with some characteristic cutoff in their transverse momenta. Besides this direct production mechanism, it is argued that the absorption effect which accounts for the nonproductive type interactions between the two nucleon-systems should also be included. Furthermore, in the context of rising total cross section, it is well known that this absorption mechanism when applied to the MP-like model avoids the violation of Froissart bound. These among other things, led us to investigate in detail the absorbed multiperipheral-like model with particles being produced independently.

In the overlap function, the main feature associated with the independent emission parameterization is the dominance of the nucleon contribution. This together with absorption enables us to describe simultaneously many features of the elastic and multiparticle data: these include the rising of total cross section, the slow rise of the slope parameters at the ISR energies, details of the differential cross sections and the gross feature of the inclusive p_T-distribution, etc.

Our expectation on the rise of the total cross section differs from some of the contemporary point of views.[15] The latter attributes this rise to be a threshold or some transient phenomena and eventually the total cross section will

be leveling off, or oscillating. In the present model once the power c is determined to be positive, the cross section is predicted to rise indefinitely. Similar conclusion has previously been reported by Cheng and Wu[16] in the context of the impact picture model which is the extract of their QED model for high energy hadron collisions. The main difference between their model and the present one is in the fundamental multiparticle production mechanism. Their model predicts a multiplicity distribution which deviates substantially from a Poisson distribution. We have not been unable to fit the multiplicity distribution within their general framework, even with the inclusion of clustering effects. The parameters λ_1 and B_1 used in the present work, as we have demonstrated predicts the gross feature of the inclusive data. A similar comparison with their model is not available at this stage.

Finally, in our calculations so far the longitudinal exclusive information is concerned, only the momenta $\bar{x}_\pi$ and $\bar{x}_N$ are involved. Further details of the longitudinal exclusive distribution have not been specified. Also we have made simplifying assumption by choosing process-A among the three production processes of (8). It is intriguing to ask, as the next step, whether with some proper choice of the exclusive p_L-distributions and further detail account for processes involved, one can achieve an overall description of pp collisions at high energies.

Footnote

A. The background Regge pole amplitude is given by

$$R(t) = [-\beta_+ (e^{-i\pi\alpha(t)} + 1) + \beta_- (e^{-i\pi\alpha(t)} - 1)]\, E^{\alpha(t)-1}\, e^{\alpha t} \quad .$$

This is for pp. For $\bar{p}p$ one replaces β_- by $-\beta_-$.

For our fits, the parameters are $\beta_+ = 9.41\ \text{GeV}^{-2}$, $\beta_- = 4.34\ \text{GeV}^{-2}$, and $\alpha = 0.7\ \text{GeV}^{-2}$.

Figure Captions

Fig. 1. The pp and $\bar{p}p$ total cross section for incident laboratory energy from 5 to 10^5 GeV/c. Solid curves are model predictions. The dashed curve represents diffractive term alone. I corresponds to IE-case, and II MP-case. For data points, see refs. 12 and 13.

Fig. 2. The slope parameter B(t) for pp differential cross section in the energy region s = 5 to 2 x 10^5 GeV^2. Theoretical curves shown are computed at t = 0 and t = -0.325 GeV^2. I corresponds to IE-case, and II MP-case. Data points as shown are divided into two groups: one with $|t| < 0.1$ and the other with $0.15 < |t| < 0.5$. See ref. 12.

Fig. 3. The ratio of the real part to the imaginary part of the pp and $\bar{p}p$ forward amplitude from 5 to 10^5 GeV/c. Solid curves are model predictions. The dashed curve represents diffractive contribution alone. I corresponds to IE-case, and II MP-case. Data points are for pp only. See ref. 12 for detail references.

Fig. 4. Schematic illustration of the unitarity diagram for inclusive p_T distribution calculation. The lines with b_X and b'_X can be either pion or nucleon.

Fig. 5. Pion and proton transverse momentum distributions. Solid curve is the predicted proton p_T^2 distributions and the dashed curve is the predicted pion p_T^2 distribution. Data points of nucleon distribution at a mean value x = 0.8 (0.7 to 0.9): NAL 303 GeV/c; x, o, □ are at 11.8 + 11.8, 15.4 + 15.4 and 22.5 + 22.5 GeV ISR energies by CHLM collaboration. The data points Δ and ∇ are at 1060 GeV/c and x = 0.85 to 0.95 respectively also by CHLM collaboration. The curve with crosses shows the experimental pion inclusive p_T^2 distribution at 23.2 + 23.2 GeV ISR energy and x = 0, from Saclay-Strasbourg collaboration. For the data, see ref. 14.

References

1. C. B. Chiu and K. H. Wang, Phys. Rev. D8, 2929 (1973).
2. C. B. Chiu, R. J. Gleiser and K. H. Wang, Diffractive Amplitude Based on Absorbed Multiperipheral-like Model and the Rising Total Cross Section, University of Texas (Austin) preprint, CPT 34 (1973).
3. C. B. Chiu and K. H. Wang, Absorption Formalism for Multiparticle Production and the Inclusive Transverse Distribution, University of Texas (Austin) preprint (1974).
4. D. Amati, A. Stanghellini and S. Fubini, Nuovo Cimento 26, 6 (1962); L. Bertocchi, S. Fubini and M. Tonin, ibid. 25, 626 (1962); G. F. Chew, M. L. Goldberger and F. E. Low, Phys. Rev. Letters 22, 208 (1969); G. F. Chew and A. Pignotti, Phys. Rev. 176, 2112 (1968); C. E. De Tar, Phys. Rev. D3, 128 (1971); F. Zachariasen, Physics Report C2, 1 (1971).
5. L. Van Hove, Rev. Modern Phys. 36, 655 (1964).
6. A. Bassetto, M. Toller and L. Sertorio, Nucl. Phys. B34, 1 (1971); E. H. de Groot and T. W. Ruijgrok, Nucl. Phys. B27, 45 (1971); E. H. de Groot, Nucl. Phys. B48, 295 (1972); D. Siver and G. H. Thomas, Phys. Rev. D6, 1961 (1972); B. R. Webber, Nucl. Phys. B43, 541 (1972); D. K. Campbell, Phys. Rev. D6, 2658 (1972).
7. G. Giacomelli, Proceedings of the 14th Int. Conf. on High Energy Physics, Vol. 3, Chicago-Batavia, 1972 (hereon referred to as paper G), p. 266; Pisa-Stony Brook collaboration, Phys. Letters 44, 119 (1973); Rome-CERN collaboration, Phys. Letters 44, 112 (1973).

8. (a) J. W. Chapman et al, Phys. Rev. Letters 29, 1686 (1972); G. Charlton et al., ibid. 29, 515 (1972); F. T. Dao et al., ibid. 29, 1627 (1972). (b) R. S. Panvini, ed., Proceedings on Experiments on High Energy Particle Collisions-1973, Vanderbilt, 1973. See articles by P. Slattery, p. 1 and by J. Whitmore, p. 14.

9. C. P. Wang, Phys. Rev. 1463 (1969); B. R. Webber, Nuclear Phys. B43, 541 (1972); E. L. Berger, D. Horn and G. H. Thomas, ANL preprint, ANL/HEP 7240 (1970); W. R. Frazer, R. D. Peccei, S. S. Pinsky and C.-I. Tan, Phys. Rev. D7, 2647 (1973); C. J. Hamer, Phys. Rev. D7, 2723 (1973).

10. (a) F. S. Henyey, Phys. Letters 45B, 363 (1973); ibid. 45B, 469 (1973); (b) R. Hwa, Phys. Rev. D8, 1331 (1973); (c) C. J. Hamer and R. F. Peierls, Phys. Rev. D8, 1358 (1973).

11. N. Byers and C. N. Yang, Phys. Rev. 142, 976 (1966); T. T. Chou and C. N. Yang, Phys. Rev. 170, 1591 (1968); H. B. Nielsen and P. Olesen, Phys. Letters 43B, 37 (1973).

12. The pp data.

(1) σ_T. 6-22 GeV/c: W. Galbraith et al., Phys. Rev. 138B, 913 (1965); 15-60 GeV/c: S. P. Denisov et al., Phys. Letters 36B, 415 (1971); 300-1500 GeV/c: see also ref. 7.

(2) Re/Im. 5, 7 GeV/c: A. R. Clyde, Ph.D. Thesis, U. C. Berkeley, 1966; 8 GeV/c: A. E. Taylor et al., Phys. Letters 14, 54 (1965); 10, 19 and 26 GeV/c: G. Bellettini et al., Phys. Letters 14, 164 (1965); 9-70 GeV/c: G. G. Beznogikh et al., Phys. Letters 39B, 411 (1972). 300-500 GeV/c: U. Amaldi et al., Phys. Letters 43B,

231 (1973). See also paper G of ref. 7, p. 286.

(3) Slope parameter. Data are from Fig. 14 of paper G of ref. 7, p. 288.

13. The $\bar{p}p$ total cross section data.

6-8 GeV/c: W. Galbraith et al., Phys. Rev. 138B, 913 (1965); 20-65 GeV/c; J. V. Allaby et al., Phys. Letters 30B, 500 (1969).

14. The inclusive transverse momentum distribution.

(1) The proton data: F. T. Dao et al., PP Interactions at 303 GeV/c, in Proceedings on Experiments on High Energy Particle Collisions, edited by R. S. Pavini (AIP, New York, 1973), p. 54, Fig. 11. The CHLM data quoted here are from CERN-Holland-Lancaster-Manchester collaboration.

(2) The pion data: M. Banner et al., Saclay-Strasbourg collaboration, Phys. Letters 41B, 547 (1972).

15. G. F. Chew and D. R. Snider, Phys. Letters 31B, 75 (1970); F. Zachariasen, Review talk given at the NAL conference on Diffractive Phenomena, 1973, Caltech preprint; A. Capella and M. S. Chen, Phys. Rev. D8, 2097 (1973); D. Siver and von Hippel, ANL preprint, 1973; M. Suzuki, University of California at Berkeley preprint, 1973; T. K. Gaisser and Chung-I Tan, Brown University preprint, 1973.

16. H. Cheng and T. T. Wu, Quantum Electrodynamics at High Energies, Int. Symp. on Electron and Photon Interactions at High Energies, Cornell University, p. 148. See also previous papers quoted therein: H. Cheng, J. K. Walker and T. T. Wu, Phys. Letters 44B, 97 (1973); 44B, 283 (1973).

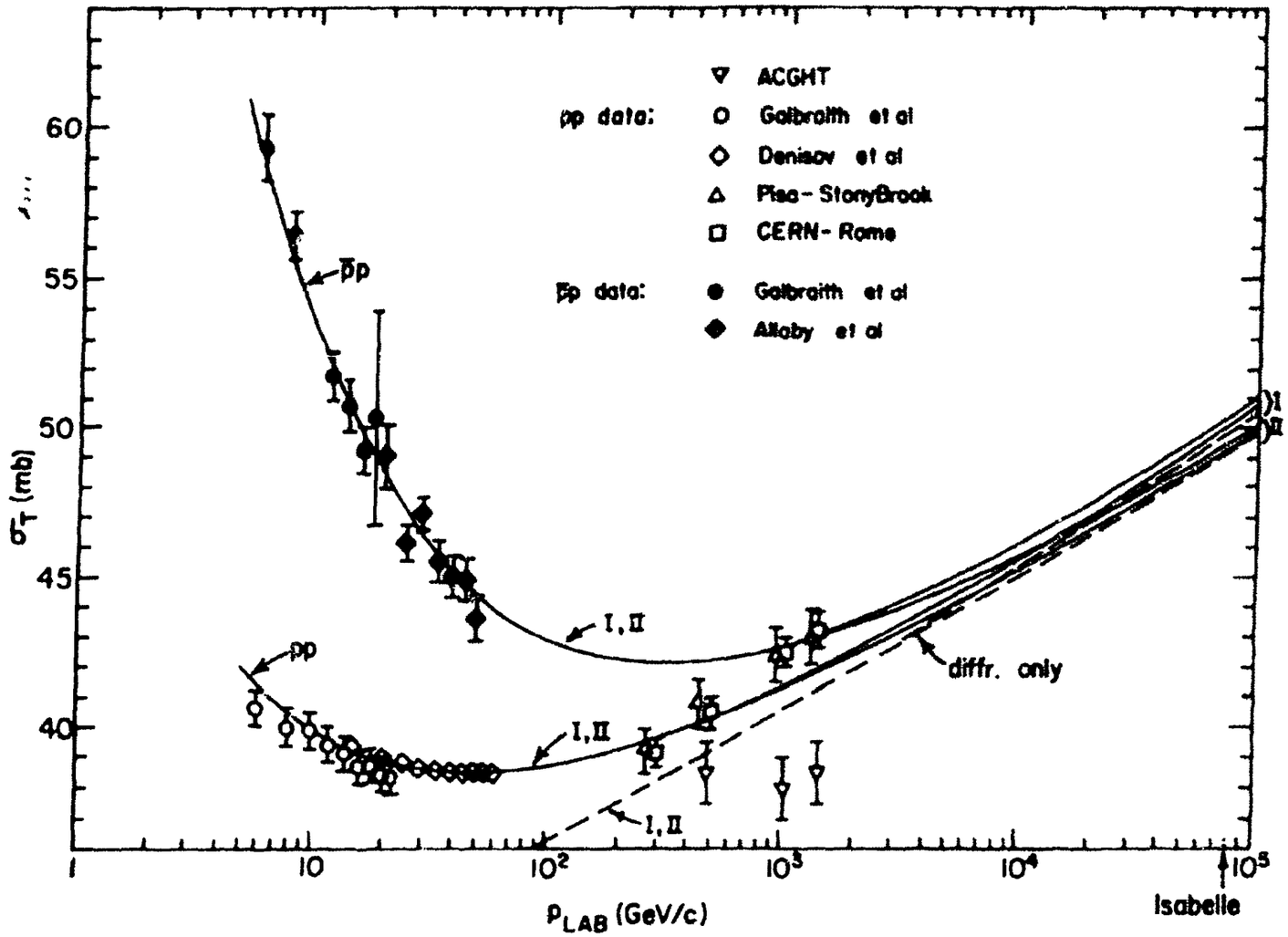
ACGHT
pp data:
Galbraith et al
Denisov et al
Pisa - StonyBrook
CERN - Rome
p̄p data:
Galbraith et al
Alkaby et al
p̄p
pp
I, II
I, II
I, II
diffr. only
60
55
50
45
40
σT (mb)
1
10
10²
10³
10⁴
10⁵
Isabelle
PLAB (GeV/c)

(FIGURE 1)

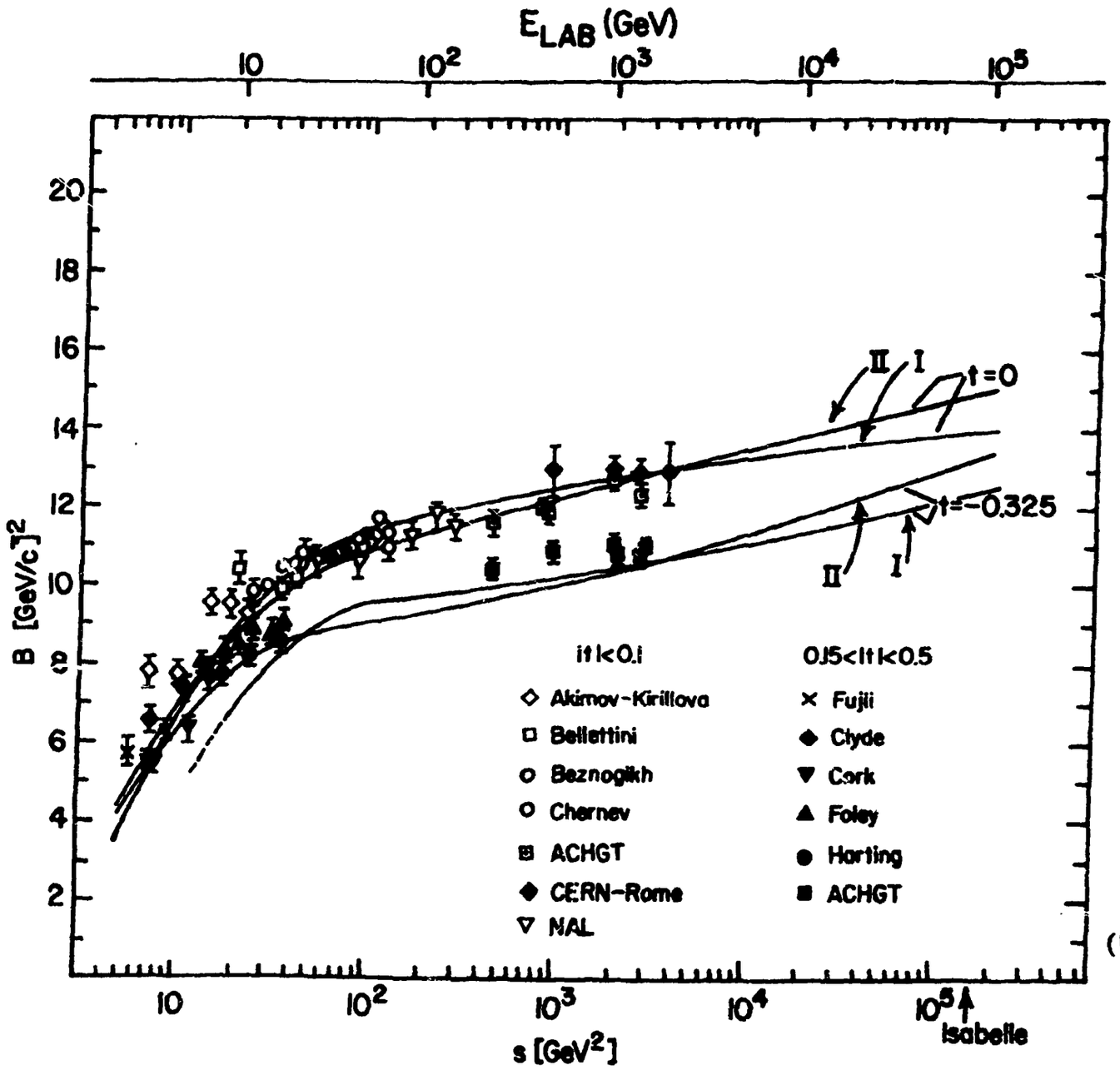
E_LAB (GeV)
10
10^2
10^3
10^4
10^5
B [GeV/c]^-2
20
18
16
14
12
10
8
6
4
2
II
I
t=0
t=-0.325
II
I
|t|<0.1
0.15<|t|<0.5
Akimov-Kirillova
Bellettini
Beznoglikh
Chernev
ACHGT
CERN-Rome
NAL
Fujii
Clyde
Cork
Foley
Herting
ACHGT
10
10^2
10^3
10^4
10^5
Isabelle
s [GeV^2]

(FIGURE 2)

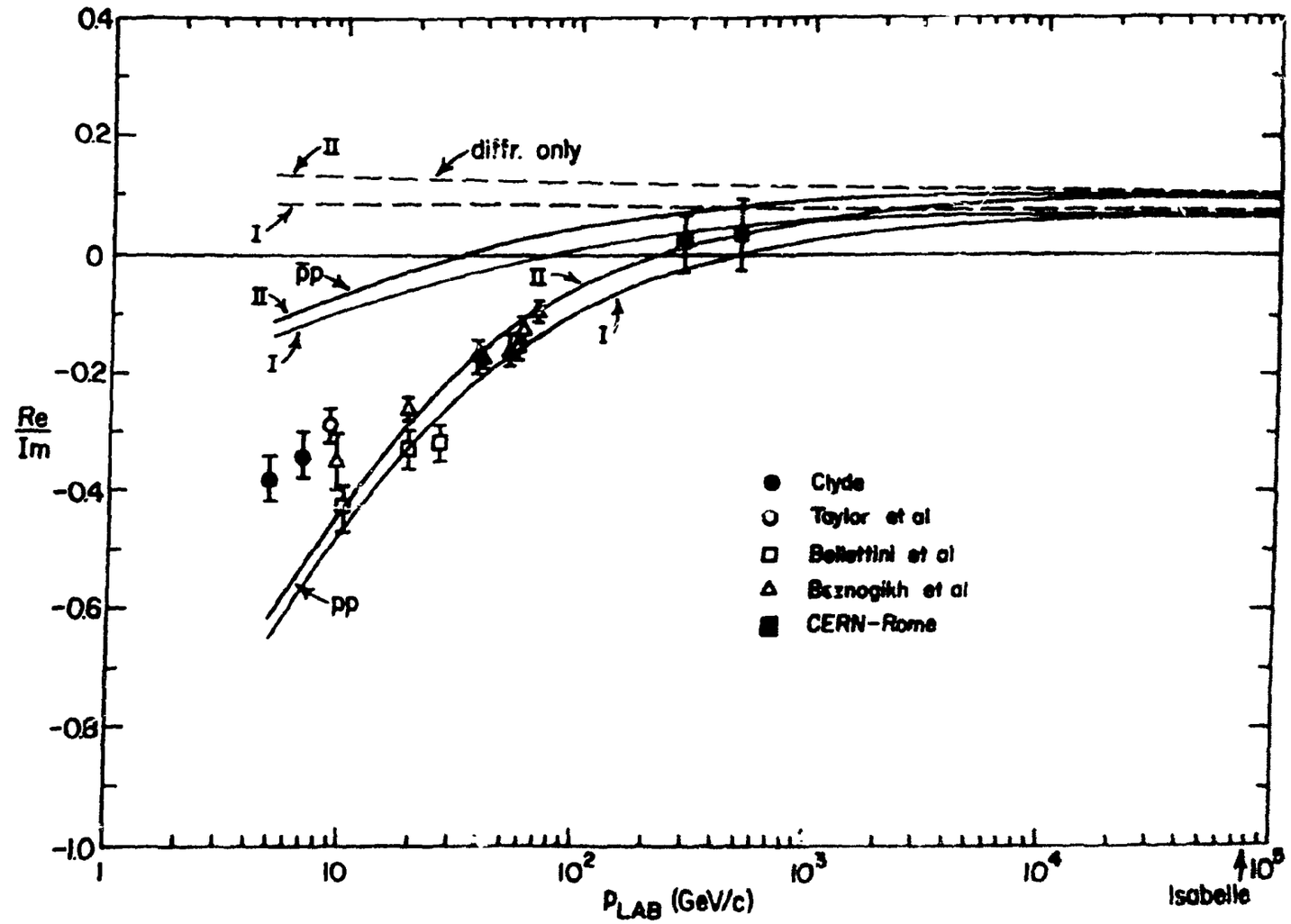
0.4
0.2
0
-0.2
-0.4
-0.6
-0.8
-1.0
Re/Im
II
diffr. only
I
p̄p
II
I
II
I
pp
Cyde
Taylor et al
Bellettini et al
Baznogikh et al
CERN-Rome
1
10
10²
10³
10⁴
10⁵
Isabelle
P_LAB (GeV/c)

(FIGURE 3)

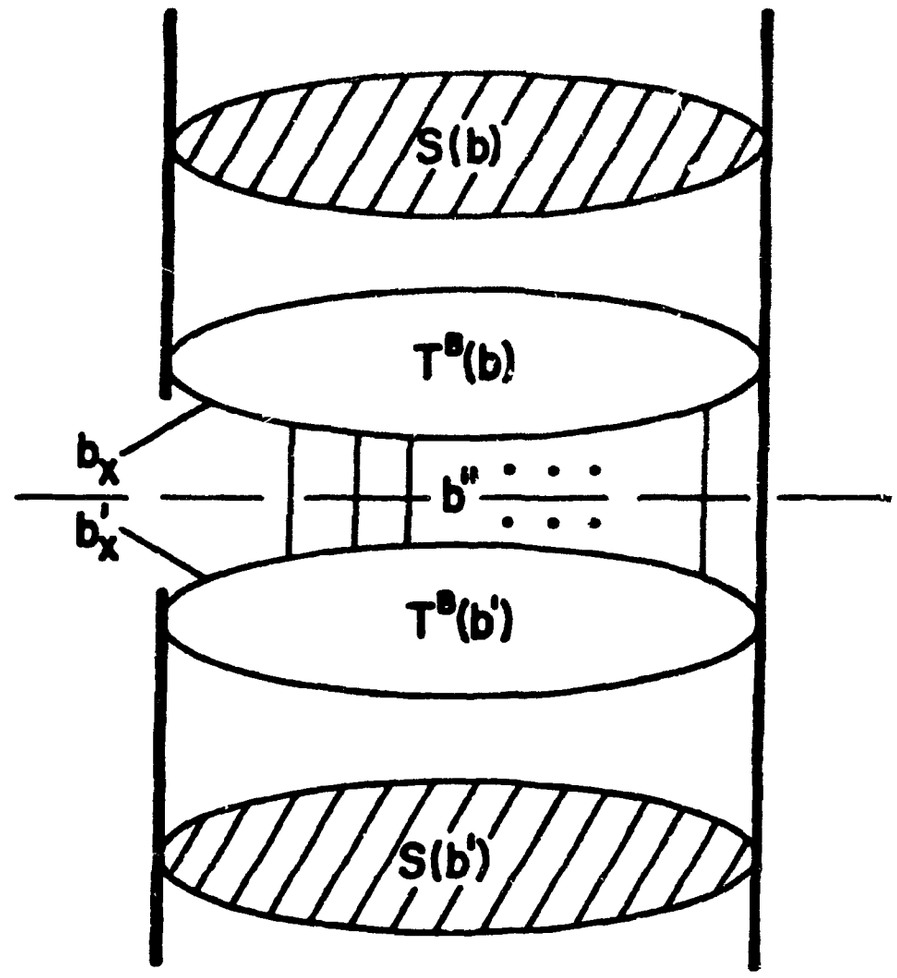

(FIGURE 4)

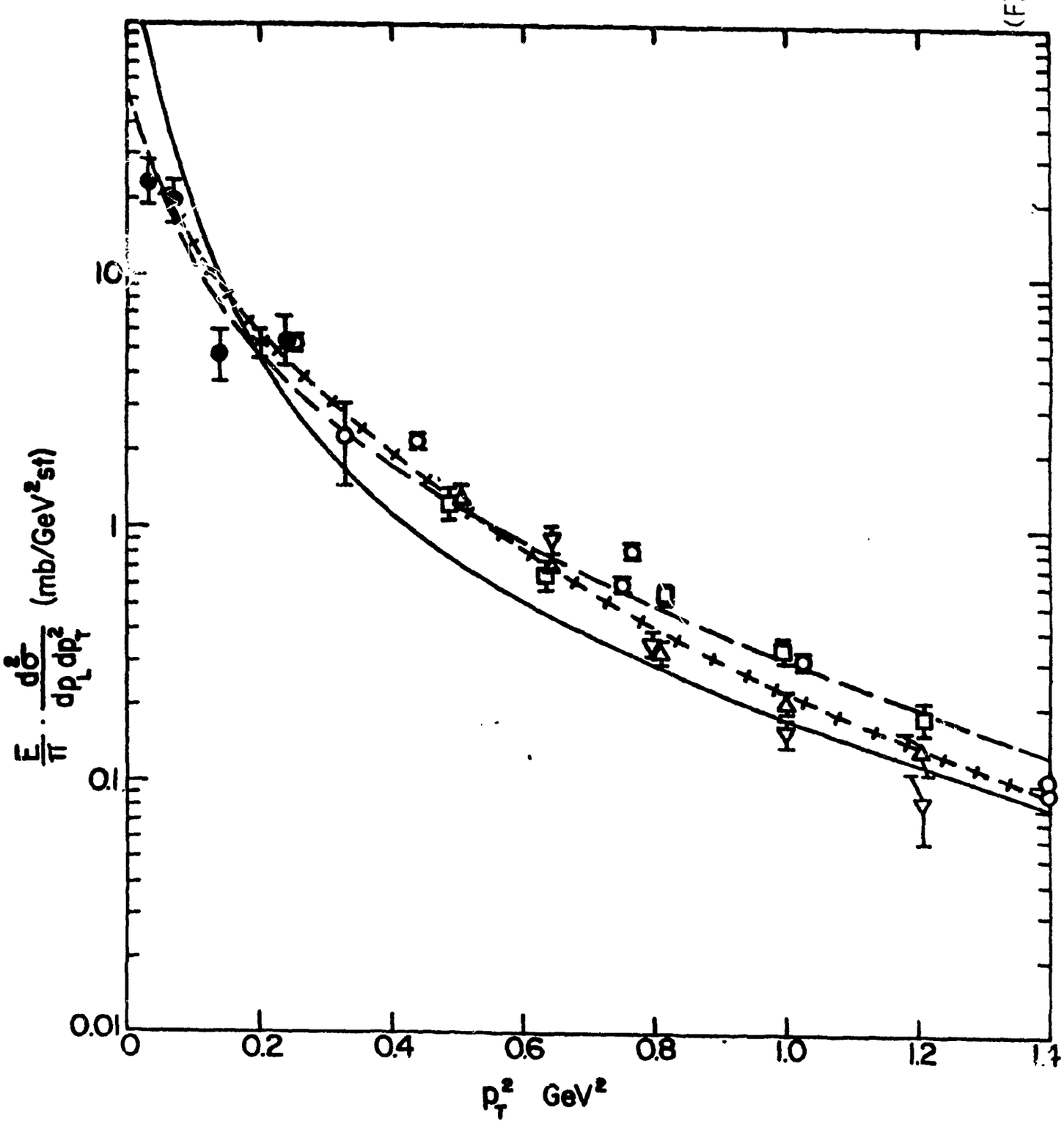
10
1
0.1
0.01
0
0.2
0.4
0.6
0.8
1.0
1.2
1.4
$\frac{E}{\pi}\cdot\frac{d^2\sigma}{dp_L\,dp_T^2}$ (mb/GeV^{2}st)
p_T^2 GeV^2

(FIGURE 5)